AAPS PharmSciTech

AAPS PharmSciTech 2000; 1 (1) article 2
(http://www.pharmscitech.com)

Liposome-Based Formulations for the Antibiotic Nonapeptide Leucinostatin A: Fourier Transform Infrared Spectroscopy Characterization and In Vivo Toxicologic Study

Submitted: January 1, 2000 ; Accepted: March 1, 2000

Maurizio Ricci[1*], Paola Sassi[2], Claudio Nastruzzi[1], Carlo Rossi[1]

[1]Institute of Chimica e Tecnologia del Farmaco, in Department of Chimica e Tecnologia, Università degli Studi, 06123 Perugia, Italy

[2]Laboratory of Physical Chemistry of the Department of Chemistry, Università degli Studi, 06123 Perugia, Italy

ABSTRACT Leucinostatin-A is a nonapeptide isolated from *Paecilomyces marquandii, Paecilomyces lilacinus* A257, and *Acremonium sp.*, exerting remarkable phytotoxic, antibacterial (especially against Gram-positive) and antimycotic activities. With the aim to find alternative formulation for in vivo administration, a number of Leucinostatin-A–loaded liposomal formulations have been prepared and characterized. Both large unilamellar vesicles and multilamellar vesicles consisting of synthetic and natural lipids were evaluated. In addition, to determine the nature of peptide-membrane interactions and the stability of liposomes loaded with Leucinostatin-A, a Fourier Transform Infrared Spectroscopy study was performed. The results suggest that the mode of interaction of the peptide is dependent on its concentration, on bilayer fluidity, and on liposome type. Finally, the LD_{50} of both free and liposome-delivered Leucinostatin-A was determined in mice. These results suggest that the incorporation of Leucinostatin-A into liposomes may result in decreased Leucinostatin-A toxicity, as the intraperitoneal administration of Leucinostatin-A–loaded liposomes reduced the LD_{50} of Leucinostatin-A 15-fold.

KEYWORDS: Liposomes; Leucinostatin-A; Thermotropic Phase Transition; Fourier Transform Infrared Spectroscopy, Preformulation, LD_{50}

*)**Corresponding Author:** Maurizio Ricci; telephone: +39-075-5855125; facsimile: +39-075-5847469; e-mail: riky@unipg.it

INTRODUCTION

Leucinostatins are a class of nonapeptides isolated from different microorganisms, namely *Paecilomyces marquandii* [1-3], *Paecilomyces lilacinus* A257 [4], and Acremonium sp. [5].

These compounds are particularly interesting since they exert remarkable phytotoxic, antibacterial (especially against Gram-positive), and antimycotic activities [1-3]. The mechanism of action of Leucinostatin-A (Leu-A) (**Figure 1**), the most abundant component of this family, is based on the inhibition of the mitochondrial ATP synthesis [6] and of different phosphorylation pathways [7].

Leu-A conformational studies, using circular dichroism and x-ray, correlated the biologic activity of the peptide to its backbone folding [8, 9]. This finding, the amphoteric character of Leu-A, and the consideration that peptides with similar structure rich in amino-isobutyric acid units can interact with biologic membranes [10], gave rise to the hypothesis that Leu-A could bind to phospholipid bilayers. This hypothesis is supported by the fact that Leu-A promotes the transport of mono- and divalent cations through the plasma membranes of mouse thymocytes [11]. However, molecular details on the mechanisms by which the peptide enters the membrane bilayer remain largely unknown.

An understanding of the molecular events responsible for Leu-A lipid membrane interactions could be useful for designing liposome-based delivery systems for the in vivo administration of Leu-A and related compounds. This would require elucidation of the possible conformational

and dynamic perturbations induced by the peptide on phospholipid vesicles (liposomes) by Fourier Transform Infrared Spectroscopy (FTIR).

Although this class of peptides represents a potentially useful group of antimicrobial agents because of their high biologic activity, their therapeutic usefulness is strongly limited by the low LD_{50}, ranging from 0.8 mg/Kg (i.v.) to 1.2 mg/Kg (i.p.) and to 5.4 mg/Kg (oral) [12].

Liposomes offer a formulation strategy for overcoming the toxicity problems, while maintaining the biologic activity. It is well known that amphiphilic drugs are entrapped more efficiently than polar drugs in liposomes, and it has been suggested that they can be incorporated directly into the liposome lipid matrix [13].

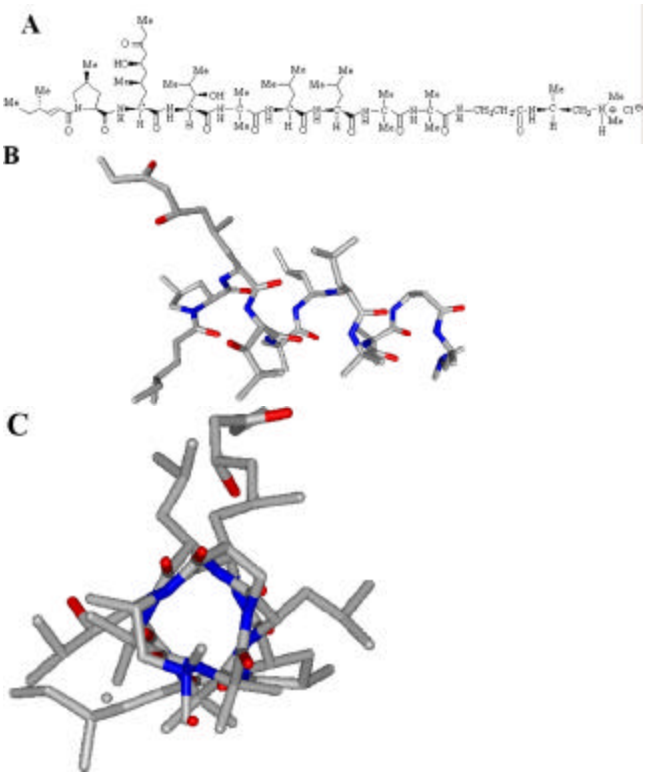

Figure 1: Chemical structure (A) and molecular model (B, C) of Leu-A. The perspective views are nearly perpendicular to the helix axis (B) and along the helix axis (C).

In this respect, development of an efficient and stable liposomal formulation for Leu-A transport requires an understanding of how the physical-chemical properties (that is, stability) of liposomes could be affected by the peptide.

The aims of the paper are a) to prepare and characterize a number of liposome-based formulations to choose the most suitable, b) to understand the molecular events responsible for Leu-A–lipid membrane interactions by means of FTIR, and finally c) to evaluate the toxicity of the liposome-based formulations.

FTIR spectral features of phospholipids in dry film state, liposomes in aqueous dispersion (both multilamellar vesicles (MLVs) and large unilamellar vesicles (LUVs), Leu-A in the dry film state, and finally Leu-A in solvents of different polarities were investigated as well. The effects induced by Leu-A on phospholipid CH_2 center of gravity (CG) and bandwidth (BW) have been assessed.

MATERIALS AND METHODS

Materials

Leu-A·HCl was obtained from cultural broth benzene extracts of *Paecilomyces marquandii* Massee (Hughes) and purified by extensive flash chromatographies on Silica Gel column as elsewhere reported [14]. Colorless crystals of Leu-A·HCl were obtained by crystallization from acetone and/or ethyl acetate.

CD_3OD (99.9 atom %D), D_2O (99.9 atom %D), CCl_4, $CDCl_3$ (99.9 atom %D), octanol, and lipids were purchased from Sigma Chemicals Co. (St. Louis, MO, USA). Purity of lipids was checked by thin-layer chromatography (TLC) using Silica Gel plates as stationary phase from E. Merck, (Darmstadt, Germany) and $CHCl_3/CH_3OH/H_2O$ (65:25:4) as mobile phase.

Development of the chromatogram, performed with Dragendorff reagent, showed one sharp spot at appropriate RF. All other reagents and solvents were of the highest purity available.

Preparation of Liposomes

MLVs were prepared by the film method properly modified accordingly with their use as follows:

a. CH_3Cl solutions containing phospholipids and Leu-A (at proper molar ratio) were poured into 50 mL round bottom flasks and placed on a Büchi T-51 rotating evaporator (Flawil, Switzerland). Rapid evaporation of the organic solvent, carried out under a stream of nitrogen over the gently warmed solutions (20-40°C), resulted in the deposition of thin films onto the flask walls. Dry lipid films were maintained overnight under reduced pressure to remove traces of organic solvent. Finally, appropriate amounts of D_2O under nitrogen atmosphere, to perform FTIR, or of buffer solutions, for all other purposes, were added yielding 45 mM phospholipid final concentrations. Films were hydrated, by shaking in a Gallenkanp orbital incubator (Fisons Instruments, Crawley, UK) at 10°C above the gel to liquid-crystalline phase transition temperature (Tm) of the employed lipids, until homogeneous white milky suspensions formed (approximately 1 hour). MLV suspensions were slowly cooled down to room temperature and stored under nitrogen at 4°C.

b. Phospholipid films were prepared as reported above. Hydration was accomplished by adding one tenth of the final buffer volume and the dispersions were shaken at 10°C above Tm at 140 rpm. After 1 hour incubation, dispersions were left at room temperature and shaken overnight. The following day, equal volumes of the remaining buffer were added in four portions at 10°C above Tm. Shaking was performed between each addition.

LUVs were prepared according to the Hope technique [15] by extruding (10 cycles) MLV suspensions (prepared as reported above) through a 0.2 µm Nucleopore polycarbonate filter (Costar Corporation, Cambridge, MA, USA) mounted on a LiposoFast® mini-extruder (Avestin Inc., St. Ottawa, Canada) fitted with two 0.5 mL syringes. Extrusions were carried out at 10°C above lipid Tm and a nitrogen atmosphere was used when hydration was performed with D_2O. All LUV suspensions were slowly cooled down to room temperature and stored at 4°C.

Characterization of Liposomes

Immediately after preparation, all LUV dispersions were checked for possible aggregation problems by visual inspection. Thereafter, in order to determine liposome mean diameter and polydispersity, quasi elastic light scattering spectroscopy (QELSS) measurements were performed using a standard laser light multiangle Brookhaven spectrometer equipped with an Argon-Ion laser and a 78 channel BI 2030AT multi-bit, multi-tau autocorrelator (Brookhaven Instruments Co., New York, NY, USA). The Laser was operated at 514.5 nm using a 90° angle between incident and scattered beams. Samples were prepared by diluting 10 µl of liposomal suspension with 2 mL of deionized water previously filtered through a 0.2 µm pore size Acrodisc LC 13 PVDF filter (Pall-Gelman Laboratory, Ann Harbor, MI, USA). During the experiment, samples were maintained in a refractive index matching liquid (toluene) at 20°C. The data reported represent the average of four measurements and the error was calculated as standard deviation (±SD). Polydispersity values, as a measure for dispersion size homogeneity, ranging from 0.0 for a completely homogeneous dispersion, to 1.0 for a completely heterogeneous system, are reported as well. Liposome morphologic analyses were carried out by transmission electron microscopy (TEM), with a Philips EM 400T microscope (Eindhoven, NL), after negative staining of the sample with phosphotungstic acid solution (0.5%).

High-Pressure Liquid Chromatography Analyses of Leu-A

Leu-A analytical determination was performed by reverse phase **high-pressure liquid chromatography** (HPLC) using a Hewlett Packard model HP 1050 chromatograph (W-7517 Waldbronn, Germany) and an endcapped Delta-Pack (Waters, Milford, MA, USA)

reversed phase column (C18, 100 Å, 300x3.9 mm). Elution was performed in an isocratic manner using, as mobile phase, a mixture of acetonitrile/isopropanol/15mM triethylammonium phosphate (TEAP) buffer solution (52.5:42:10.5). Leu-A was monitored with a spectrophotometric detector set at 220 nm. Calibration curve for HPLC assays of Leu-A, concentration range 5-300 μ g/ml, had a correlation coefficient greater than 0.99. Leu-A retention time was 5.28 minutes.

Leu-A Loading

Leu-A content in liposome dispersions was determined by HPLC after dissolution of Leu-A–loaded liposomes in CH_3OH. Free Leu-A was determined in supernatants after ultracentrifugation of suspensions using a Beckman Optima™ Series TL (Palo Alto, CA, USA) ultracentrifuge with a TLA 100.4 rotor (85000 x g for 2 h at 4°C). Leu-A content was calculated by the difference between total and free Leu-A in suspensions and in supernatants, respectively. Loading was expressed as percentage of the Leu-A initial amount.

Fourier Transform Infrared Spectroscopy Analyses

All spectra were recorded with a Bruker IFS113v spectrometer (Karlsrue, Germany) equipped with a deuterated triglycine sulfate (DTGS) pyroelectric detector. For each spectrum, 256 interferograms were collected to ensure an adequate signal-to-noise ratio; interferograms were co-added, apodized with a triangular function, and Fourier transformed to give a resolution of 2 cm^{-1}. Spectral manipulations were performed with GRAMS32 (Galactic Industries, Salem, NH, USA) and Bruker OPUS2 data manipulation software.

Spectra of phospholipid alone or mixed with Leu-A were recorded in dry film state and as liposome suspensions.

Dry films were obtained by spreading 100-200 mL of a $CHCl_3$ stock solution (40 mM) on one face of a CaF_2 crystal, then carefully evaporating the solvent until a homogeneous film was obtained. Residual solvent traces were removed under reduced pressure (25mm Hg) for 4 hours. Samples treated in this manner were considered anhydrous, since no water absorption was detected in the Leu-A IR spectra.

Liposomal samples were prepared by sealing, under nitrogen atmosphere, 50 μl of each dispersion between two 25 mm CaF_2 crystals separated by a 50 μm polyethylene spacer. The sealed samples were placed into a demountable temperature-controlled cell (Spectra-Tech Inc., Stamford, CT, USA).

Spectra, obtained over the mid-infrared region between 4000 and 900 cm^{-1}, were collected every 1°C between 8 and 50°C, while maintaining isothermal conditions (±0.25°C) by using an Omega (Stamford, CT, USA) temperature controller. Temperatures were monitored by a copper-constantan thermocouple placed against the edge of the cell window. During spectral scans, the interferometer chamber was constantly purged with dry nitrogen to flush any water vapor and carbon dioxide from the atmosphere. Leu-A anhydrous samples, alone or mixed with phospholipids, were cast as films using the same procedure.

D_2O, CD_3OD, $CDCl_3$, CCL_4 and octanol Leu-A solutions, as well as Leu-A KBr pellets, were prepared following the usual procedure.

Band positions of both CH_2 asymmetric (2950-2900 cm^{-1}) and symmetric (2880-2830 cm^{-1}) stretching vibrational modes were determined by calculating the CG of each band at 95% of the band height. Full BWs were calculated at 75% of the band height [16]. A curve fitting procedure was used for quantitative assessment of individual components in the broad contours of peptide amide I band, and was performed using GRAMS32 software. In all cases, the examined bands were reproduced by Lorentzian-Gaussian profile.

Acute Toxicity

Charles River (Wilmington, MA, USA) CD2F1 male mice (18-22 g in weight), were treated via i.p. route with free Leu-A solutions and peptide-loaded liposomes dispersions. Groups of five mice were injected with scalar doses (0.6, 0.8, 1.0, 1.8, 2.4, 4.8, 9.6, 14.9, 20.25 mg/kg) of Leu-A alone or of Leu-A–loaded liposomes; all experiments were performed in triplicate. Mice were

under observation for toxic effects or death immediately after injection, then daily for seven days. Dose-mortality curves (**Figure 5**) show that DMPC:CH:DMPG liposomes were particularly effective in reducing the toxicity (15 fold) of the peptide.

RESULTS AND DISCUSSION

Leu-A Structure and its Fourier Transform Infrared Spectroscopy Characteristics

The molecular structure of Leu-A [9] resembles a corkscrew shape, having a positive charge on the (2S)-N,N-dimethylpropane-1,2-diamine moiety, a substantially hydrophobic helical body and two arms made by the hydrophilic (2S, 4S, 6S) -2-amino-6-hydroxy-4-methyl-8- oxodecanoic acid, and the hydrophobic (4S,2E)-4-methylhex-2-enoic acid (MHA) respectively (**Figure 1**).

Leu-A FTIR spectra in different systems, namely CD_3OD, $CDCl_3$, CCl_4 or octanol solutions or in KBr pellets or in the dry film state (**Figure 2A -and 2B**), have been recorded and the main peaks assigned (**Table 1**). The data showed no significant changes in the spectra with the exception of that performed in KBr, wherein a shift toward higher wavelengths was observed. The spectrum recorded in dry film was used as reference.

To better characterize possible Leu-A conformational changes induced by the environment, the amide I peak, in the 1690-1620 cm^{-1} interval, was examined [17]. Because this vibrational band is particularly sensitive to variations of the secondary structure [18], the careful fitting of its components has been performed (**Figure 3** and **Table 2**) to attempt to identify possible conformational variations of the peptide depending on its environment. In this respect, all spectra revealed the presence of more conformers, of which the α -helical conformation was the predominant in more apolar environments, in agreement with previous findings [17]. Moreover, since the peptide does not have a β -structure, it was postulated that the bands at 1627-1638 and 1671-1675 cm^{-1} could be due to the presence of short, extended chains before and after the α -helical cylinder [18].

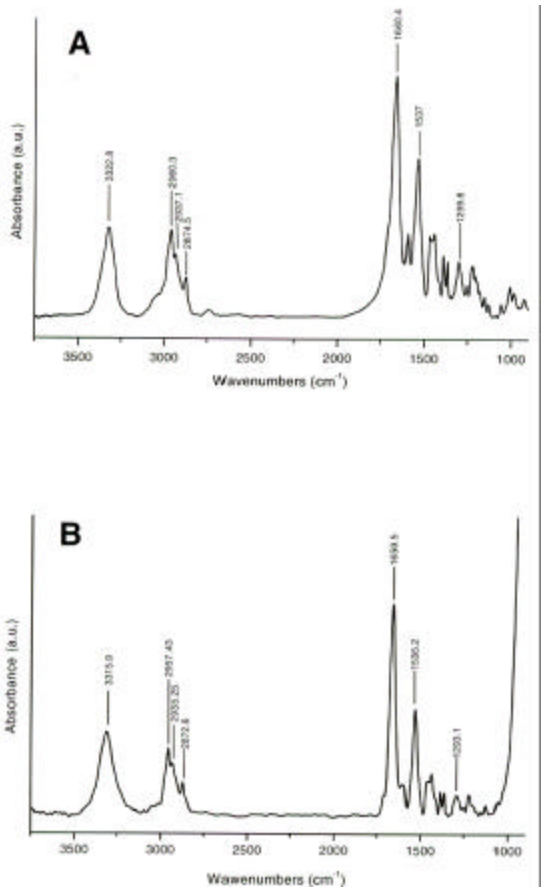

Figure 2: Infrared spectra of Leu-A in KBr (A) and as dry film (B).

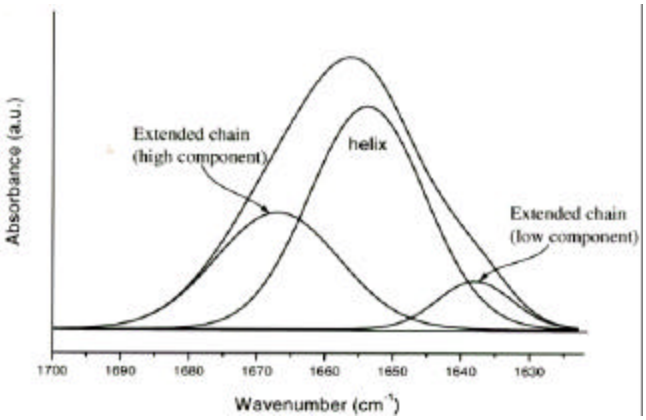

Figure 3: The amide I band contour with the best fitted individual component bands for Leu-A in CDCl3.

Table 1. Assignments of the major peaks present in the spectrum of Leu-A in different systems.

Functional group	Wavenumbers (cm^{-1})					
	KBr	Dry film	CCl_4	$CDCl_3$	octanol	CD_3OD
NH str.	3322	3315	3318	3316	-	-
CH_3 asym. str.	2960	2957	2959	2958	-	-
CH_2 asym. str.	2937	2935	2936	2935	-	-
CH_3 sym. str.	2874	2872	2872	2871	-	-
C=O str. (Amide I)	1660	1659	1659	1656	1655	1658
C-N str. (Amide II)	1537	1535	1536	1535	1538	-
Amide III	1299	1293	1294	1293	1298	-

Table 2. Frequency assignments (cm^{-1}) and fractional areas (in %) of the Leu-A amide I components in different systems.

	a-helix	Extended chains	
		Low components	High components
KBr	1658.5 (58.5%)	1636.1 (6.2%)	1679.3 (35.3%)
Dry film	1657.2 (84.4%)	-	1674.2 (15.6%)
CCl_4	1658.6 (67.7%)	1644.6 (10.7%)	1668.9 (21.5%)
$CDCl_3$	1653.8 (58.7%)	1638.0 (8.2%)	1667 (33.0%)
Octanol	1654.8 (73.0%)	-	1670.3 (27.0%)
CD_3OD	1654.8 (36.0%)	1640.9 (17.6%)	1668.4 (46.4%)

Leu-A–Loaded Liposomes

Leu-A–loaded LUV, analyzed by TEM (**Figure 4**), confirmed that the extruded liposomal suspensions consisted mainly of homogeneous LUV. Since the average size and size distribution represent two of the major parameters for liposome characterization and prediction for their in vivo behavior in terms of biodistribution and pharmacokinetics, QELSS measurements were performed. Dimension of LUVs was determined, as well as the influence of increasing concentration of Leu-A on liposome size. The mean diameters of MLVs are not reported since, as expected, the high polydispersity of this type of vesicles did not render reliable and reproducible results.

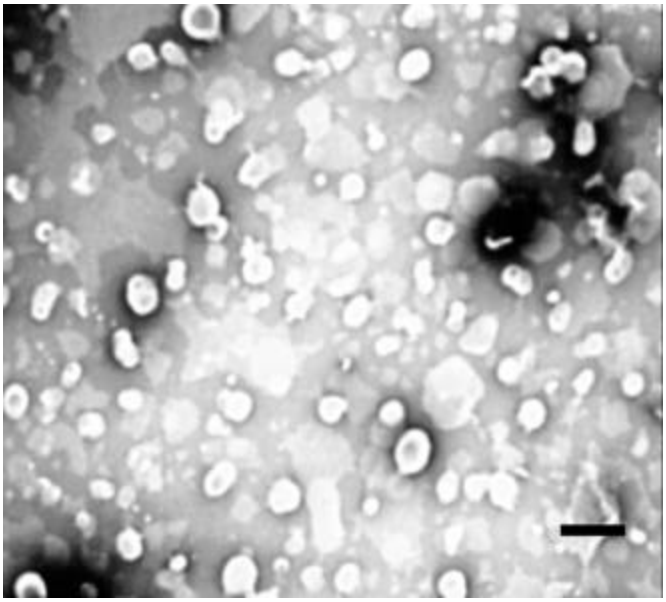

Figure 4. Transmission electron micrograph of Leu-A loaded DMPC unilamellar liposomes, produced by extrusion of multilamellar vesicles through 0.2 mm filters. Bar corresponds to 250 nm.

Table 3. Incorporation of Leu-A in MLV liposomes with different lipid composition

Composition and molar ratio	% of loaded Leu-Amean ± SD
DSPC	37.6 ± 0.9
DSPC:CH (10:2.5)	44.5 ± 1.0
DSPC:DPPG (10:1)	19.9 ± 1.5
DSPC:CH:DPPG (10:2.5:1)	55.6 ± 0.2
DHPC	51.4 ± 1.2
DHPC:CH (10:2.5)	12.5 ± 1.2
DHPC:DHP (10:1)	51.8 ± 1.2
DHPC:CH:DHP (10:2.5:1)	53.5 ± 0.2
DMPC	24.2 ± 0.9
DMPC:CH (10:2.5)	8.5 ± 1.1
DMPC:PS (10:1)	26.4 ± 0.5
DMPC:CH:PS (10:2.5:1)	6.7 ± 1.0
DMPC:DMPG (10:1)	48.7 ± 0.9
DMPC:CH:DMPG (10:2.5:1)	40.5 ± 1.0
DPPC	11.5 ± 1.3
DPPC:CH (10:2.5)	8.7 ± 1.0
DPPC DPPG (10:1)	10.3 ± 1.3
DPPC:CH:DPPG (10:2.5:1)	9.2 ± 1.0
Egg PC	2.1 ± 1.4
Egg PC:CH	5.4 ± 1.2
Egg PC:DMPG	3.8 ± 1.6
Egg PC:CH:DMPG	6.2 ± 0.9

For instance, empty dimyristoyl-phosphatidylcholine (DMPC) vesicles displayed a mean diameter of 210 nm, clearly reflecting the pore size of the filter used for their extrusion. The Leu-A loading caused a decrease of vesicle size, which was reduced to 110-130 nm by adding concentrations of peptide, from 1:0.016 to 1:0.2 (mol/mol, lipid:Leu-A). Polydispersity values and liposome mean diameters (**Figure 5**) indicate that the best formulation is reached when Leu-A/DMPC molar ratio is 0.064.

To evaluate the loading capacity of liposomes, different lipid compositions were tested. Both natural (egg phosphatidylcholine (egg PC)) and synthetic phospholipids were assayed and the effect of (a) chain length, (b) presence of cholesterol (CH), (c) presence of dimyristoylphosphatidylglycerol (DMPG) or phosphatidylserine (PS) and finally (d) ether lipids, were investigated. From the results (**Table 3**) some considerations could be drawn. The use of lipids with low phase transition temperature (Tm), such as egg PC, yielded a very poor loading capacity that never exceeded 7%, a result also observed when CH or DMPG were

present. Phospholipids with a higher Tm, such as DSPC, produced liposomes with the highest Leu-A loading (19.9%-55%). The inclusion of ether lipids, such as dihexadecylphosphatidyl-choline (DHPC), afforded relatively high Leu-A loading yields which, in many cases, exceeded 50%. The presence of CH produced contradictory results. When added to DSPC, the Leu-A liposome loading capacity is augmented. In contrast when CH is combined with DMPC or DHPC, the Leu-A loading is strongly reduced. This apparently anomalous behavior might be explained because (1) in liposomes with very high Tm the presence of CH renders the membrane more fluid and hence the inserting of the guest molecule is favored, and (2) in liposomes with lower Tm, the presence of CH stabilizes the membrane only to a certain extent, but not enough to prevent guest Leu-A leakage.

Effect of Leu-A on Thermotropic Behavior of Liposomes

From FTIR spectra of DMPC in dry film state (**Figure 6**), C-H stretching vibration modes, observed in the 3100-2800 cm^{-1} region (asymmetric and symmetric CH_2 bands, respectively, located at around 2920 and 2850 cm^{-1}), were chosen because they represented the strongest signals, and were thus very useful to study guest molecule-phospholipid bilayer interactions. It is well known that alterations in band stretching, in term of both position and width, indicate conformational order changes, before, during, and after phospholipid main gel to liquid-crystalline transition due either to a change in temperature or to the presence of guest molecules. The CH_2 stretching frequencies are primarily sensitive to the degree of conformational disorder, which increases in response to the introduction of gauche rotamers, while BWs broaden as a result of rate and amplitude increases of CH_2 group motion [16].

To avoid interpretation errors of bands absorbing in the 3000-2800 cm^{-1} region, the infrared (IR) spectra of free liposomes, a Leu-A/DMPC mixture and of free Leu-A were compared. To get best band resolution and univocal results, dry films of these samples were preferred over the use of D_2O-hydrated samples. This

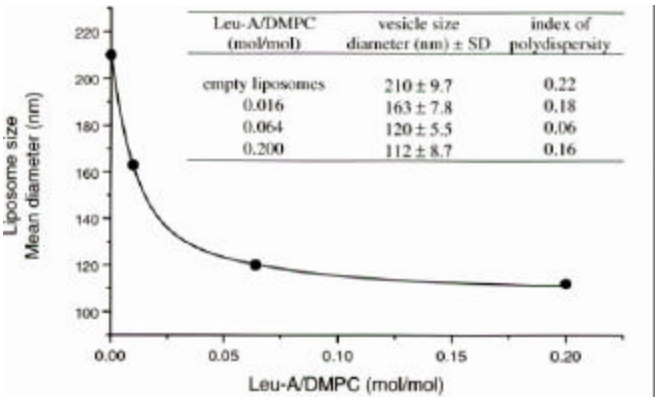

Figure 5: Effect of Leu-A on DMPC LUV size and polydispersity.

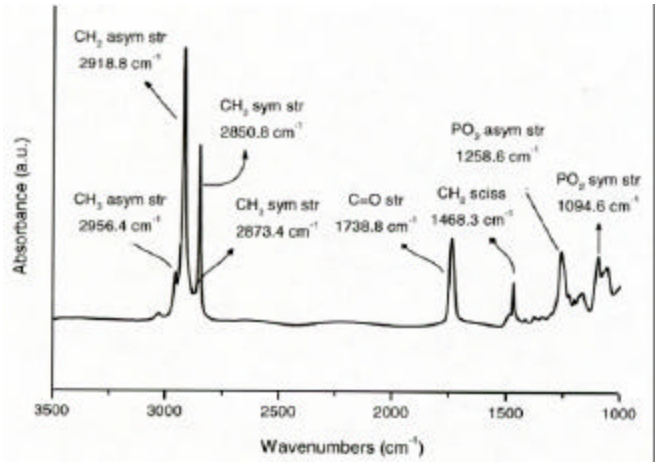

Figure 6: Infrared spectrum of DMPC in dry film state

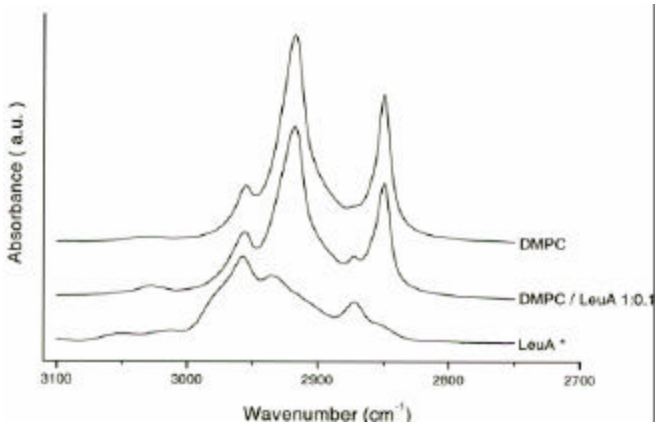

Figure 7: Infrared spectra of DMPC, LeuA/DMPC mixture and of free Leu-A in dry film state (*) intensity x 10

choice was made since Leu-A is very poorly soluble in D_2O and the IR spectrum of Leu-A and liposomes, in D_2O or in dry film state, are nearly superimposable. The spectrum of lipid–Leu-A mixture (1:0.1 mol/mol)

clearly showed that the phospholipid -CH_2 bands partially overlap with those of the peptide and therefore could give rise to some calculation errors of the lipid absorption bands (**Figure 7**). For this reason, only symmetric CGs and BWs were used to detect alterations induced by the peptide on lipid membranes. In addition, monitoring the band at 2850 cm^{-1}, rather than that at 2920 cm^{-1}, was preferred in order to avoid the broad Fermi resonance band which occurs at ca. 2950 cm^{-1}.

Plots of CGs and BWs versus temperature of DMPC-MLVs in the presence of increasing Leu-A concentrations (**Figure 8**) showed that, in the range 8-20°C (gel phase), CG values of all DMPC/Leu-A mixtures were only slightly lower than those measured for DMPC vesicles. This finding suggests that only minor interactions between the peptide and the lipid membranes occurred. Above the main transition temperature, no remarkable shifts of the CG values were observed, suggesting that the peptide does not alter the acyl chain conformation (**Figure 8A**). As previously observed [19], this behavior was attributed to Leu-A molecule aggregations in small clusters, which interfere only slightly with membrane acyl chains without any detectable CG shifts.

Figure 8: Effect of Leu-A on symmetric center of gravity (A, C) and bandwidth (B, D) of multilamellar (A, B) and unilamellar (C, D) liposomes constituted by DMPC. Leu-A was used at the following molar ratio. DMPC/Leu-A 1:0.016 (triangles); 1:0.06 (diamonds) 1:0.2 (squares) (mol/mol). For comparison, data relative to empty DMPC liposomes (circles) are also reported.

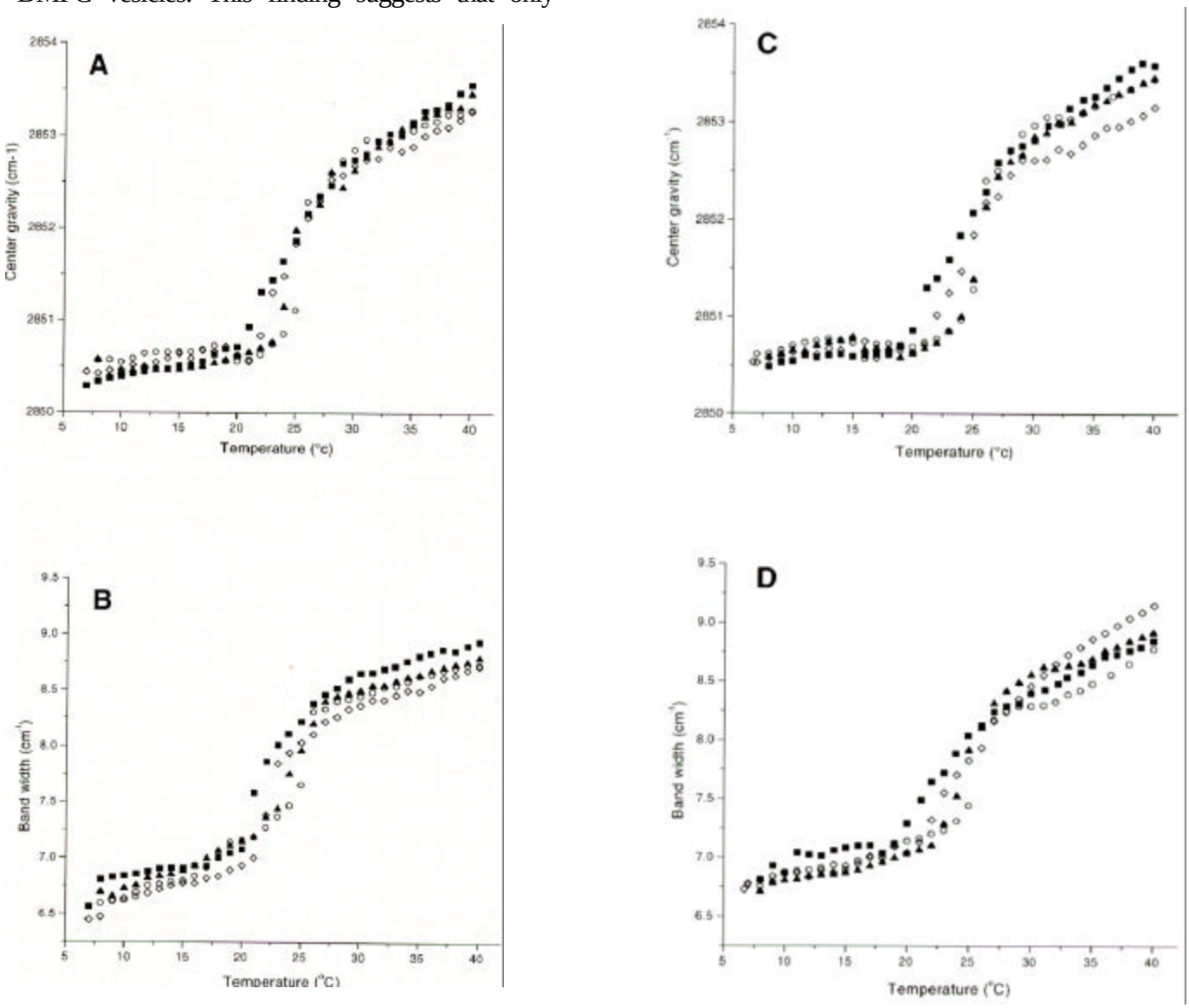

It is postulated that Leu-A, when the membrane is in a gel phase, faces the hydrophilic portion of the phospholipid head-groups, while the hydrophobic MHA residue of the molecule partially penetrates into the hydrocarbon chain region close to the polar/non polar interface. However, when the membrane is in the liquid-crystalline phase, the peptide can penetrate more deeply into the hydrophobic core, with possible formation of Leu-A rich (clusters) and Leu-A poor domains.

More importantly, Leu-A gave rise to an evident broadening of the gel to liquid crystalline phase transition (Tm), the mid-point of which is progressively reduced from about 26°C, in the case of pure DMPC, to 23°C, in the case of DMPC/Leu-A mixture (1:0.2). This behavior indicated a decrease in co-operativity between adjacent phospholipid chains.

Further confirmation of peptide-lipid bilayer interactions came from the temperature dependence variations observed for the CH_2 stretching BWs (**Figure 8B**). It is known that BWs are sensitive to vibrational and reorientation motions of the lipid CH_2 groups, depending upon their environment [16]. In this case, lipid melt broadening and midpoint lowering were in agreement with those above observed (**Figure 8A**), while chain mobility increased only in the presence of higher peptide concentrations, especially in the liquid crystalline phase. No significant differences were observed between MLVs (**Figure 8A and 8B**) and LUVs (**Figure. 8C and 8D**), except for the BW behavior above Tm. In fact, in LUV, the presence of Leu-A produces a greater increase of the BW values. This suggests that the presence of the peptide increases the alkyl chain mobility due to the different lamellar organization in MLVs and LUVs, the latter being less packed and hence more easily perturbed by the presence of guest molecules, especially when in the liquid-crystalline phase.

Acute Toxicity

A series of experiments was performed in order to test which liposomal formulation could produce beneficial effects on the in vivo acute toxicity of the peptide, with the exception of those which provided very poor Leu-A loading. All tested formulations, when injected via i.p into mice, displayed different toxicity reduction (**Table 4**). Mice were under observation for death immediately after i.p. injection, then at any time up to seven days. The best results were obtained with DMPC:DMPG (10:1, mol/mol) and DMPC:CH:DMPG (10:2.5:1, mol/mol/mol) formulations. Dose-mortality curves (**Figure 9**) show that DMPC:CH:DMPG liposomes were particularly effective in reducing the toxicity (15-fold) of the peptide.

Table 4. LD_{50} of Leu-A in MLV liposomes with different lipid composition

Composition and molar ratio (i.p.)	Approximate LD_{50} (mg/kg)
DSPC	1.2
DSPC:CH (10:2.5)	2.1
DSPC:DPPG (10:1)	1.2
DSPC:CH:DPPG (10:2.5:1)	4.2
DHPC	1.2
DHPC:CH (10:2.5)	1.9
DHPC:DHP (10:1)	1.2
DHPC:CH:DHP (10:2.5:1)	5.8
DMPC	2.5
DMPC:Chol (10:2.5)	n.t.
DMPC:PS (10:1)	1.2
DMPC:CH:PS (10:2.5:1)	n.t.
DMPC:DMPG (10:1)	6.5
DMPC:CH:DMPG (10:2.5:1)	17.5
DPPC	n.t.
DPPC:CH (10:2.5)	n.t.
DPPC DPPG (10:1)	n.t.
DPPC:CH:DPPG (10:2.5:1)	n.t.
Egg PC	n.t.
Egg PC:CH	n.t.
Egg PC:DMPG	n.t.
Egg PC:CH:DMPG	n.t.
Leu-A•HCl	1.2

n.t. = not tested

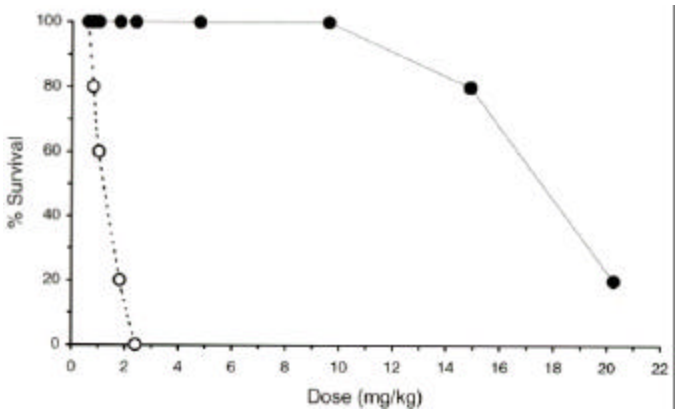

Figure 9: Dose-mortality curves for free (opened circles) and liposome delivered (filled circles) Leu-A injected *via* i.p. in CD2F1 male mice. Liposomes consisted of DMPC:CH:DMPG (10:2.5:1 mol/mol/mol).

CONCLUSION

FTIR indicated that Leu A and phospholipid vesicles do interact (although not strongly) with liposomes. However, when the peptide is mixed with liposomes up to a 1:0.2 (lipid to Leu-A) molar ratio, no appreciable instability problems, by visual inspection or by photon correlation spectroscopy, were noticed. The capacity of liposomes to reduce the in vivo acute toxicity of the antimicrobial peptide suggests that lipid-based formulations represent a promising improvement for the possible preclinical use of the peptide. It should be emphasized that only acute toxic effects of liposome formulations have been tested. In this respect, it is well known that the bioavailability of drugs in liposomal formulations is a function of size; thus, the toxicity of MLVs and of LUVs could be significantly different over time. In order to answer to this question, a series of experiments is in progress to optimize liposomal formulations and to find which composition minimizes the toxic and other unwanted effects while maintaining the efficacy of this potential drug.

ACKNOWLEDGMENTS

This work has been supported by Grants of the Italian MURST (Ministry for the University) and CNR (National Research Council).

REFERENCES

1. Casinovi CG, Rossi C, Tuttobello L, Ricci M. The structure of Leucinostatin C. A minor peptide from *Paecilomyces marquandii*. Eur J Med Chem. 1986;21:527-528.

2. Rossi C, Ricci M, Tuttobello L, Casinovi CG, Radics L. Leucinostatin D, a novel peptide antibiotic from *Paecilomyces marquandii*. J. Antibiotics. 1987;40:130-133.

3. Rossi C, Ricci M, Tuttobello L, Casinovi CG, Radics L, Kajtar-Peredy M. Leucinostatins H and K, two novel peptide antibiotics with tertiary amine-oxide terminal group from *Paecilomyces marquandii*: isolation, structure and biological activity. J. Antibiotics 1987;40:714-716.

4. Fukushima K, Arai T, Mori Y, Tsuboi M, Suzuki M. Studies on peptide antibiotics, Leucinostatins II. The structures of Leucinostatins A and B. J. Antibiotics 1983;36:1613-1630.

5. Strobel G A, Torczynski R, Bollon A. *Acremonium sp.* - a Leucinostatin A producing endophyte of european yew (*Taxus baccata*). Plant Sci. 1997;128:97-108.

6. Shima A, Fukushima K, Arai T, Terada H. Dual inhibitory effects of the peptide antibiotic leucinostatins on oxidative phosphorylation in mitochondria. Cell Struct Funct. 1990;15,:53-55.

7. Lucero HA, Lescano WIM, Vallejos RH. Inhibition of energy conservation reaction in chromatophores of *Rhodospirillum rubrum* by antibiotics. Arch Biochem Biophys. 1978;186:9-14.

8. Vertuani G, Falcomer C, Boggian M, et al. Structural studies of Leucinostatin A and its Boc-Aib-Leu-Leu-Aib-OMe tetrapeptide fragment. Int J Peptide Protein Res. 1988;33:162-170.

9. Cerrini S, Lamba D, Scatturin A, Rossi C, Ughetto G. The crystal and molecular structure of the α-helical nonapeptide antibiotic Leucinostatin A. Biopolymers. 1989;28: 409-420.

10. Benedetti E, Bavoso A, Di Blasio B, , et al. Peptaibol antibiotics: a study on the helical structure of the 2-9 sequence of Amerimicins III and IV. Proc Natl Acad Sci U S A. 1982;79:7951-7954.

11. Csermely P, Radics L, Rossi C, Ricci M, Szamel M, Somorgy J. The nonapeptide Leucinostatin A acts as a weak ionophore and as an immunosuppressant on lymphocytes. Biochim Biophys Acta 1994;1221:125-132.

12. Mikami Y, Fukushima K, Arai T, Abe F, Shibuya H, Ommura Y. Leucinostatins, peptide mycotoxins produced by *Paecilomyces lilacinus* and their possible roles in fungal infection. Zbl Bakt Hyg 1984;257:275-283.

13. Cortesi R, Esposito E, Gambari R, Menegatti E, Nastruzzi C. Liposome-associated retinoids: production, characterization and antiproliferative activity on

neoplastic cells. Eur J Pharm Sci. 1994;2:281-291.

14. Vertuani G, Boggian M, Scatturin A, et al. Structure activity studies on chemically modified homologues of the antibiotic phytotoxic Leucinostatin A. J Antibiotics. 1995;48:254-260.

15. Hope MJ, Bally M, Webb G, Cullis P. Production of large unilamellar vesicles by a rapid extrusion procedure. Characterization of size distribution, trapped volume and ability to maintain a membrane potential. Biochim Biophys Acta. 1985;812:55-65.

16. Casal HL, Mantsch HH. Polymorphic phase behaviour of phospholipid membranes studied by infrared spectroscopy. Biochim Biophys Acta. 1984;779:381-401.

17. Byler DM, Susi H. Examination of the secondary structure of proteins by deconvolved FTIR spectra. Biopolymers. 1986;25:469-487.

18. Surewicz WK, Stepanik TM, Szabo AG, Mantsch HH. Lipid-induced changes in the secondary structure of snake venom cardiotoxins. J Biol Chem. 1988;263: 86-90.

19. Fresta M, Ricci M, Rossi C, Furneri PM, Puglisi G. Antimicrobial nonapeptide Leucinostatin A–dependent effects on physical properties of phospholipid model membranes. In press.